Knockdown of Filaggrin in a Three-Dimensional Reconstructed Human Epidermis Impairs Keratinocyte Differentiation

Valérie Pendaries[1,2,3], Jeremy Malaisse[4], Laurence Pellerin[1,2,3], Marina Le Lamer[1,2,3], Rachida Nachat[1,2,3,8], Sanja Kezic[5], Anne-Marie Schmitt[6], Carle Paul[1,2,3,7], Yves Poumay[4], Guy Serre[1,2,3] and Michel Simon[1,2,3]

Atopic dermatitis is a chronic inflammatory skin disorder characterized by defects in the epidermal barrier and keratinocyte differentiation. The expression of filaggrin, a protein thought to have a major role in the function of the epidermis, is downregulated. However, the impact of this deficiency on keratinocytes is not really known. This was investigated using lentivirus-mediated small-hairpin RNA interference in a three-dimensional reconstructed human epidermis (RHE) model, in the absence of other cell types than keratinocytes. Similar to what is known for atopic skin, the experimental filaggrin downregulation resulted in hypogranulosis, a disturbed corneocyte intracellular matrix, reduced amounts of natural moisturizing factor components, increased permeability and UV-B sensitivity of the RHE, and impaired keratinocyte differentiation at the messenger RNA and protein levels. In particular, the amounts of two filaggrin-related proteins and one protease involved in the degradation of filaggrin, bleomycin hydrolase, were lower. In addition, caspase-14 activation was reduced. These results demonstrate the importance of filaggrin for the stratum corneum properties/functions. They indicate that filaggrin downregulation in the epidermis of atopic patients, either acquired or innate, may be directly responsible for some of the disease-related alterations in the epidermal differentiation program and epidermal barrier function.

Journal of Investigative Dermatology advance online publication, 10 July 2014; doi:10.1038/jid.2014.259

INTRODUCTION

Atopic dermatitis (AD; OMIM #603165) is one of the most common chronic inflammatory skin diseases, affecting 15–25% of children and 3% of adults in industrialized countries (Odhiambo *et al.*, 2009; Bieber, 2012). The pathophysiology of AD is complex and involves numerous genetic and environmental factors. Clinically, AD is characterized by erythematous skin lesions, pruritis, increased transepidermal water loss, and a marked mononuclear cell infiltrate in the dermis. It was long thought that the AD primary defect resided in the immune system, leading to excessive inflammation and a secondary local epidermal barrier disruption. However, some recent studies have suggested that permeability barrier abnormality in AD is not merely a consequence but rather the ''driver'' of the disease activity, allowing antigen penetration and percutaneous sensitization (Cork *et al.*, 2006; Oyoshi *et al.*, 2009; Novak and Simon, 2011; Bieber, 2012; Kezic *et al.*, 2014). Loss-of-function mutations in the gene-encoding filaggrin (*FLG*) are the strongest and most widely replicated risk factors for the disease (Kezic *et al.*, 2014). Meta-analyses of genetic studies involving many thousands of patients have demonstrated this association, with an overall odds ratio for AD ranging from 3.12 to 4.78 (Baurecht *et al.*, 2007; Rodriguez *et al.*, 2009). Many clinical features of atopic skin have been associated with *FLG* mutations: a decrease in the levels of free amino acids in the stratum corneum (SC) (Kezic *et al.*, 2008), an increase in transepidermal water loss and SC pH (Kezic *et al.*, 2008; Jungersted *et al.*, 2010; Winge *et al.*, 2011), dryness (Winge *et al.*, 2011), and abnormal bacterial colonization (Boguniewicz and Leung, 2011).

Filaggrin is produced by granular keratinocytes as a large precursor called profilaggrin, which consists of 10–12 filaggrin repeats flanked by single N- and C-terminal domains. Profilaggrin is the major component of the keratohyalin granules. At the granular-to-cornified cell transition, profilaggrin is rapidly dephosphorylated and cleaved to generate basic filaggrin monomers and terminal domains (Dale *et al.*, 1985;

[1]*UMR5165 CNRS, Toulouse, France;* [2]*U1056 INSERM, Toulouse, France;* [3]*UDEAR, University of Toulouse, Toulouse, France;* [4]*Cell and Tissue Laboratory, URPHYM-NARILIS, University of Namur, Namur, Belgium;* [5]*Academic Medical Center, Coronel Institute of Occupational Health, Amsterdam, The Netherlands;* [6]*Pierre Fabre Dermo-Cosmétique, Toulouse, France and* [7]*University Hospital, Toulouse, France*

[8]*Present address: Greentech France, Saint Beauzire, France*

Correspondence: Michel Simon, CNRS-INSERM-UPS UMR5165, CHU Purpan, Place du Dr Baylac TSA40031, 31059 Toulouse, France.
E-mail: michel.simon@udear.cnrs.fr

Abbreviations: AD, atopic dermatitis; FLG, filaggrin gene; RHE, reconstructed human epidermis; RT-qPCR, reverse transcription-quantitative PCR; SC, stratum corneum

Received 3 December 2013; revised 14 May 2014; accepted 20 May 2014; accepted article preview online 18 June 2014

Brown and McLean, 2011). The N terminus is translocated into the nucleus where it may be involved in nuclear breakdown (Ishida-Yamamoto *et al.*, 1998; Pearton *et al.*, 2002). As for the filaggrin monomers, they associate with keratin filaments and are suspected of inducing the formation of the corneocyte fibrous matrix (Steinert *et al.*, 1981). In the cornified cells, after deimination by peptidylargine deiminases, filaggrin is degraded into free amino acids by some proteases, including caspase-14, bleomycin hydrolase, and calpain 1 (Scott *et al.*, 1982; Chavanas *et al.*, 2006; Baurecht *et al.*, 2007; Denecker *et al.*, 2008; Brown and McLean, 2011). These amino acids are thought to be critical for skin photoprotection and for the acidification and hydration of the SC (Scott *et al.*, 1982; Rawlings and Harding, 2004; Elias and Steinhoff, 2008; Brown and McLean, 2011).

To prove the importance of filaggrin and analyze its functions, filaggrin-null mice and filaggrin knockdown in organotypic human skin models have been studied. However, conflicting results have been obtained. In mice, complete filaggrin deficiency leads to dry scaly skin, SC fragility, abnormal keratin aggregation, decreased amino acid levels in the SC, altered epidermal barrier integrity, and enhanced percutaneous sensitization, but normal SC water content, conductance, and pH (Kawasaki *et al.*, 2012). *In vitro* knockdown of human filaggrin with small interfering RNA (Mildner *et al.*, 2010) or microRNA (Aho *et al.*, 2012) in two living-skin equivalent models has led to different results. In 2010, Mildner *et al.* (Mildner *et al.*, 2010) reported impaired lamellar body formation, reduced urocanic acid content in the SC, increased penetration through the SC, and increased sensitivity to UV-B-induced apoptosis, but normal keratin solubility, keratinocyte proliferation and differentiation, and SC lipid composition. In 2012, a second study showed increased thickness of the epidermis with an increase in keratin 16 expression and activation of caspase-14 (Aho *et al.*, 2012). Finally, small interfering RNA knockdown of filaggrin in HaCaT cells grown at the air–liquid interface showed reduced expression of loricrin, E-cadherin, and occludin (Yoneda *et al.*, 2012).

To better understand the effect of filaggrin deficiency on keratinocytes in a fibroblast- and immunological cell-free context, we knocked down its expression with small-hairpin RNA (shRNA) technology in reconstructed human epidermis (RHE) on a polycarbonate filter. We particularly focused on epidermal differentiation, SC properties, and permeability barrier.

RESULTS

Filaggrin deficiency in RHE leads to a thinner epidermis, loss of keratohyalin granules, and impaired SC formation

Filaggrin expression knockdown was achieved using RNA interference in normal human primary keratinocytes, which were secondarily used to obtain RHE as previously described (Frankart *et al.*, 2012). The experiments were performed with two shRNAs targeting filaggrin (shFLGa and shFLGb) and keratinocytes obtained from three different donors. Similar levels of filaggrin expression were observed in RHE produced with keratinocytes from any of the donors (Supplementary Figure S1 online). The two shRNAs were used separately, with identical results (for comparison, some results obtained with shFLGb are shown in Supplementary Figure S2 online).

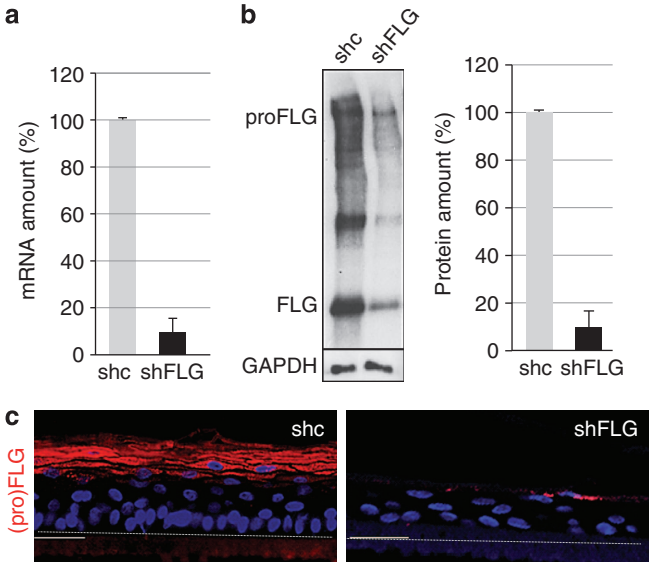

Figure 1. Expression of filaggrin is highly reduced in RHE produced with shFLG keratinocytes. (**a**–**c**) Fully differentiated shc- and shFLG-reconstructed human epidermis (RHE) were analyzed by quantitative real-time reverse-transcriptase–PCR (**a**), and by both western blotting (**b**) and immunofluorescence (**c;** in red) performed with an AHF3 antibody. Immunodetected profilaggrin and filaggrin monomers were quantified and normalized to GAPDH levels. Error bars represent the SD calculated from three experiments performed with keratinocytes from three different donors, each in triplicate. The polycarbonate filter–epidermal junction is indicated by thin lines. Bars = 50 μm.

After 10 days of culture at the air–liquid interface, fully differentiated epidermis was obtained. As previously reported (Frankart *et al.*, 2012), proper expression of keratins and differentiation markers was achieved and the SC was functionally competent. The RHE produced with keratinocytes transduced with either a control shRNA (shc-RHE) or shFLGa (shFLG-RHE) was analyzed by quantitative real-time reverse-transcriptase–PCR (RT-qPCR), and immunodetected with AHF3, a monoclonal antibody specific for filaggrin and profilaggrin, using western blotting and indirect immunofluorescence (Figure 1). In shFLG-RHE, filaggrin mRNA and protein (both profilaggrin and filaggrin monomers) amounts were decreased by 92% and 90%, respectively, compared with shc-RHE (Figure 1a and b). Immunofluorescence labeling of RHE sections showed the expression of profilaggrin in the granular layers of shc-RHE, and a marked reduction of staining in shFLG-RHE (Figure 1c).

Morphologically, shc-RHE was similar to normal human epidermis, as shown by hematoxylin–eosin staining. In contrast, shFLG-RHE appeared thinner with a reduced number of keratinocyte layers and reduced SC thickness, and a marked reduction in keratohyalin granules (Figure 2a and Supplementary Figure S3a and b online). Transmission electron microscopy analysis (Figure 2b) of shc-RHE showed keratinocyte organization and structures similar to those observed in normal human skin, including corneodesmosomes,

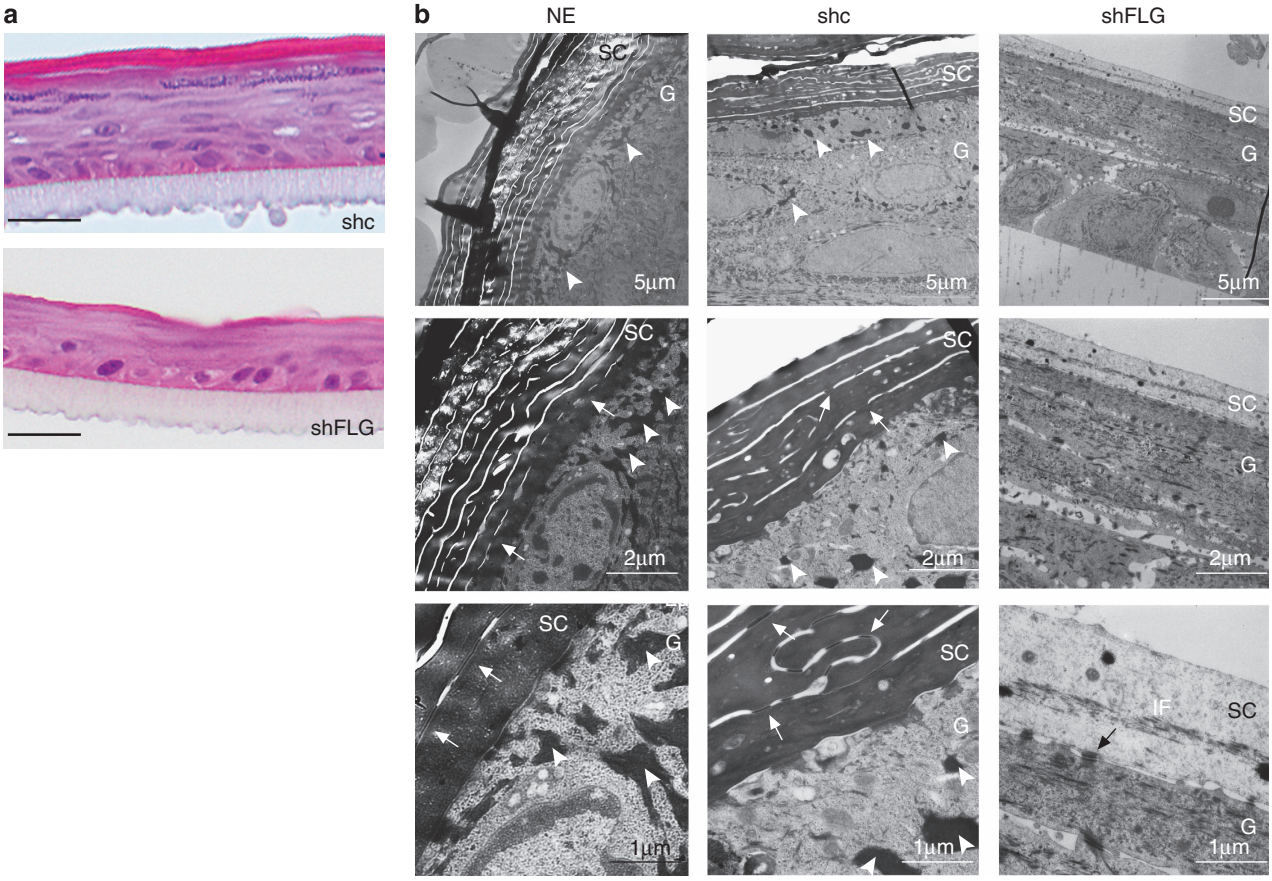

Figure 2. Filaggrin deficiency leads to altered epidermal morphology. (**a**) Sections of paraffin-embedded shc- and shFLG-reconstructed human epidermis (RHE) were stained with hematoxylin and eosin. One representative experiment of three is shown. Bars = 20 µm. (**b**) Normal epidermis (NE), shc-, and shFLG-RHE were analyzed by electron microscopy, as described in Supplementary Materials and Methods online. Corneodesmosomes (white arrows), desmosomes (black arrows), and keratohyalin granules (arrowheads) were observed. The stratum corneum (SC) and granulosum (G) are indicated. Scale bars are shown.

desmosomes, keratohyalin granules, and lamellar bodies. The ultrastructural examination of shFLG-RHE confirmed the reduction in keratohyalin granules (Supplementary Figure S3c online) and SC thickness. In addition, corneocytes displayed an unusually low electron density of their matrix, and corneodesmosomes were not observed. The analysis also indicated an apparent dilation of the extracellular spaces in the upper living keratinocyte layers. However, the desmosomes and the distribution of desmosomal proteins and E-cadherin appeared normal (Supplementary Figure S4 online). In addition, the keratinocyte proliferation before epidermal reconstruction was not modified by the down-regulation of filaggrin (Supplementary Figure S5a online), active caspase-3 was not detected (data not shown and Figure 3c), and cellular viability, as tested using a 3(4,5-dimethylthiazol-2-yl)-2,5-diphenyltetrazolium bromide (MTT) assay, was not altered (Supplementary Figure S5d online) in shFLG-RHE. However, on day 10, a slight but statistically significant reduction in Ki67 staining was observed (Supplementary Figure S5b and c online). This suggested that the reduced thickness was due to keratinocyte altered differentiation and reduced proliferation.

SC functional properties are disturbed in filaggrin-deficient RHE

To investigate the effect of filaggrin knockdown on SC permeability, we used the Lucifer yellow assay (Mildner *et al.*, 2010). The hydrophilic fluorescent dye was applied to the shc- and shFLG-RHE external surface for 6 hours on day 10. The green dye was retained in the SC of the control RHE (Figure 3a, left panel) but passed through the filaggrin-deficient RHE and markedly stained the polycarbonate filter (Figure 3a, right panel).

Amino acids derived from filaggrin degradation are thought to partly regulate the pH in the SC. Therefore, we analyzed the pH of the external surface of the RHE. Filaggrin inhibition, however, was not shown to induce any noticeable pH modifications (from 6.38 ± 0.25 to 6.49 ± 0.15; $P = 0.21$; Supplementary Figure S6 online). To know whether filaggrin reduction impacted the natural moisturizing factor, we measured the urocanic acid and pyrrolidone carboxylic acid contents of the RHE (Dapic *et al.*, 2013). HPLC analysis of RHE lysates revealed statistically significant decreases of urocanic (31%; from 5.90 to 4. 10 mmoles ml^{-1}) and pyrrolidone carboxylic (18%; from 45.83 to 37.80 mmoles ml^{-1})

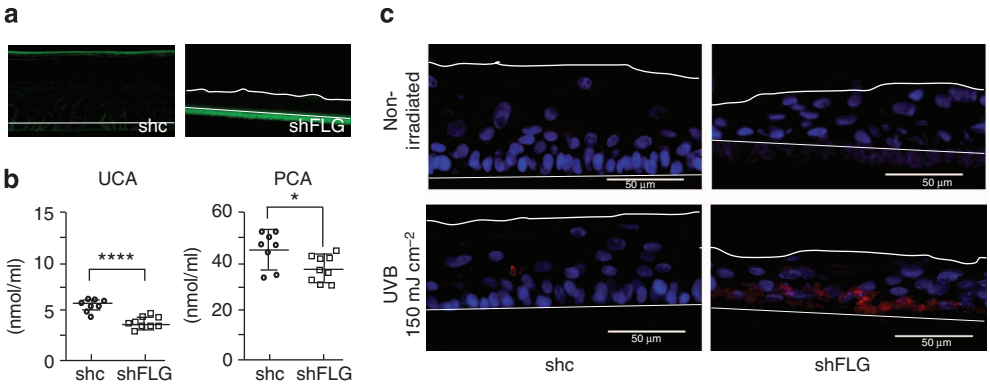

Figure 3. The stratum corneum properties of filaggrin-deficient RHE are impaired. (**a**) A solution of Lucifer yellow was applied onto the stratum corneum of the shc- and shFLG-reconstructed human epidermis (RHE) . After 6 hours, penetration of the dye was investigated using sections of paraffin-embedded tissue observed under a fluorescence microscope. The stratum corneum surface (thick line) and the polycarbonate filter (thin lines) are indicated. Bars = 20 µm. (**b**) Urocanic acid (t-UCA) and pyrrolidone carboxylic acid (PCA) amounts were quantified using HPLC in lysates of shc-RHE ($n=8$) and shFLG-RHE ($n=9$). *$P<0.05$; **$P<0.001$. Means and SE are indicated. (**c**) Shc- and shFLG-RHE were irradiated with UV-B (150 mJ cm^{-2}), and the active caspase-3 was detected using indirect immunofluorescence (in red). DNA was labeled with 4′,6′-diamidino-2-phenylindole (in blue).

acids in filaggrin knockdown RHE as compared with the control samples (Figure 3b).

Urocanic acid is suspected to protect skin against UV-B radiation (Barresi *et al.*, 2011). We therefore irradiated shc- and shFLG-RHE and detected active caspase-3 as a marker of apoptosis induction (Figure 3c). Knockdown of filaggrin resulted in an increase in caspase-3 activation, suggesting increased UV sensitivity.

Filaggrin knockdown in RHE affects the epidermal differentiation program

To study keratinocyte differentiation in RHE, we explored the expression of a panel of proteins differentially expressed in the various layers of the epidermis by western blotting and quantification of the detected bands (Figure 4a and b). We considered a change in protein immunodetection by a factor of 1.5 as significant. Compared with control RHE, the detection of the following proteins was decreased in filaggrin-deficient RHE: filaggrin-2, hornerin, keratin (K) 10, loricrin, caspase-14 (both the precursor and active forms), and bleomycin hydrolase. In contrast, the detection of corneodesmosin and claudin 1 increased. The expression of desmoglein 1/2, desmocollin 1, involucrin, K14, E-cadherin, and calpain 1 was not modified. Immunofluorescence labeling confirmed the decrease in filaggrin-2, hornerin, caspase-14, and bleomycin hydrolase detection (Figure 4c). Interestingly, the distribution of corneodesmosin was shown to be altered with little pericellular labeling observed (Supplementary Figure S4b online), in agreement with the absence of corneodesmosomes.

To determine whether the modifications of protein expression observed in shFLG-RHE were due to changes in the corresponding mRNA levels, a quantitative real-time PCR analysis was performed (Figure 4d). In comparison with control RHE samples, mRNA levels of filaggrin-2, loricrin, caspase-14, and bleomycin hydrolase were reduced in filaggrin-deficient RHE, whereas the corneodesmosin mRNA level was increased. The levels of mRNAs encoding hornerin, K10, K14, desmoglein 1, desmocollin 1, involucrin, claudin 1, E-cadherin, and calpain 1 were modified only slightly or not at all.

Procaspase-14 activation is reduced in both shFLG-RHE and atopic skin

In the shFLG-RHE, in addition to the downregulation of caspase-14, a reduction in the processing of the proform to the active form of the protease was observed (mean factor of 55.6 ± 4.4; $n=4$). To know whether this was also the case in AD, total protein extracts of normal epidermis and of the epidermis from both lesional and non-lesional skin of AD patients were analyzed by western blotting. Patients and controls without any of the four *FLG* mutations most prevalent in the European population (R501X, 2282del4, S3247X, and R2447X) were selected. The amounts of procaspase-14 and caspase-14 large subunit detected and the procaspase-14/caspase-14 ratio were then computed. Large interindividual variations were observed in the amounts of both the proform and the activated form. The amounts of procaspase-14 were increased in the lesional skin samples, as compared with non-lesional and control skin ($P=0.00987$ and $P=0.00094$, respectively). The amounts of caspase-14 seemed to be reduced in patients (both in non-lesional and lesional skin samples), but the decreases were not statistically significant (Supplementary Figure S7 online). However, as observed in the RHE, the activation of procaspase-14 was reduced in the patients (Supplementary Figure S8 online). The mean ratio of 5.06 in controls was shown to increase to 15.47 in lesional and to 11.82 in non-lesional atopic skin samples. We did not find any correlation between the reduced activation of caspase-14 and the amounts of filaggrin quantified in the epidermal extracts using western blotting (data not shown). This is not surprising as caspase-14 seems to proteolyze filaggrin fragments, already processed by another protease, rather than filaggrin monomers, at least in the mouse (Denecker *et al.*, 2008).

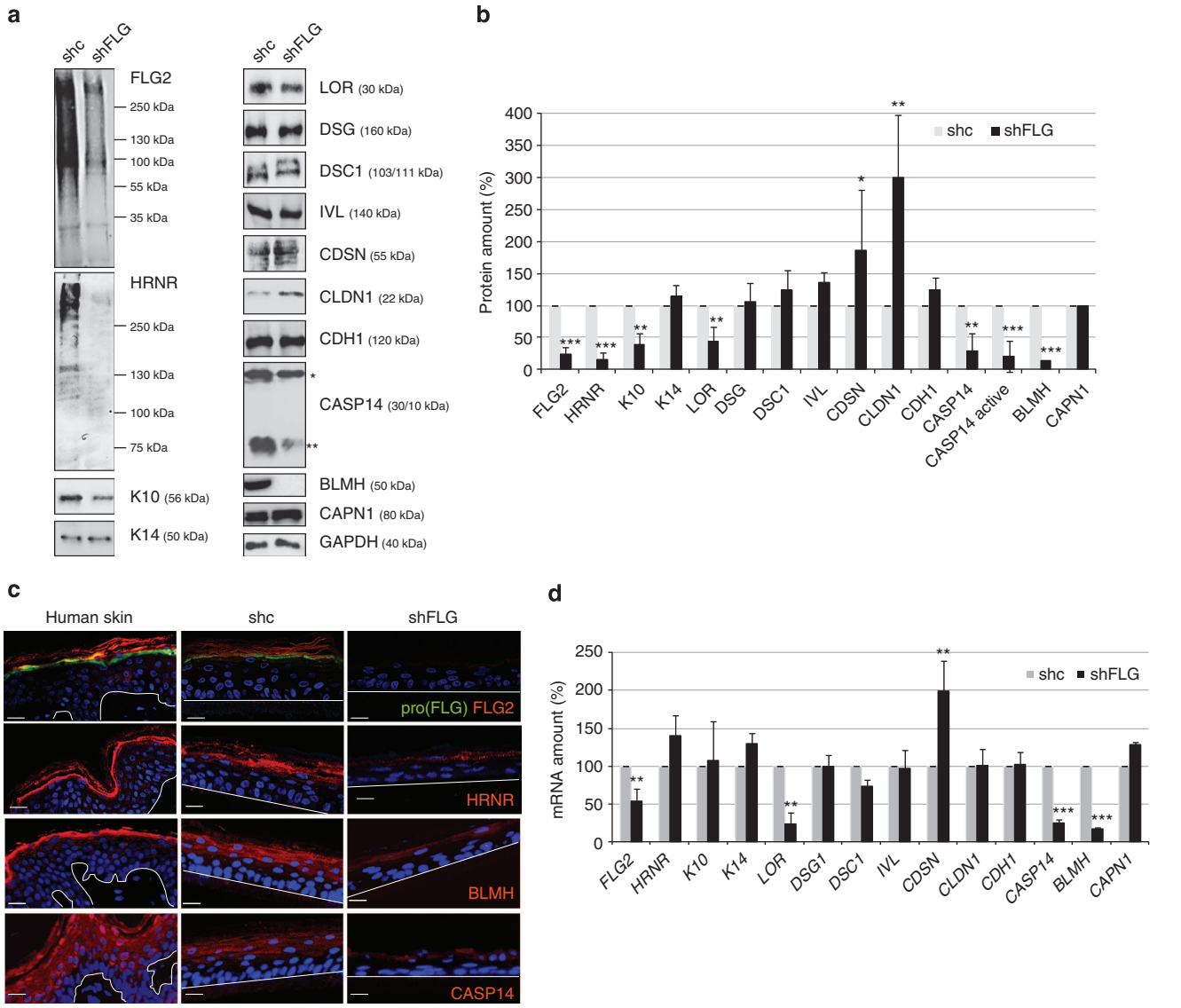

Figure 4. Filaggrin knockdown alters keratinocyte differentiation. (**a**–**d**) Expression of proteins in shc- and shFLG-reconstructed human epidermis (RHE) was either analyzed by western blotting (**a**) and quantified (**b**) or investigated by immunofluorescence staining (**c**) and quantitative real-time reverse-transcriptase–PCR (**d**). FLG, filaggrin; HRNR, hornerin; K, keratin; LOR, loricrin; DSG, desmoglein; DSC, desmocollin; CASP14, caspase-14 (both precursor (*) and active (**) forms); BLMH, bleomycin hydrolase; CDSN, corneodesmosin; CLDN, claudin; IVL, involucrin; CDH1, E-cadherin; CAPN, calpain; GAPDH, glyceraldehyde 3-phosphate dehydrogenase. Error bars represent the SD calculated as indicated in the legend of Figure 1. The polycarbonate filter– and dermo-epidermal junctions are indicated by dashed lines. Scale bars = 20 μm. $^{**}P<0.01$; $^{***}P<0.001$.

DISCUSSION

Nonsense mutations in the gene-encoding filaggrin are responsible for ichthyosis vulgaris and are frequently associated with AD (Baurecht *et al.*, 2007; Rodriguez *et al.*, 2009; Brown and McLean, 2011). Moreover, the expression of filaggrin and other major constituents of the SC is decreased in adult AD patients, both in lesional and non-lesional skin, irrespectively of their *FLG* genotype (Pellerin *et al.*, 2013). However, the real impact of filaggrin deficiency on the epidermal barrier is not completely known. To answer this question we used RHE as a 3D model produced with keratinocytes only, without any other cell types. We report here that filaggrin knockdown by RNA interference technology in RHE extensively alters keratinocyte differentiation, SC integrity, and SC function. In particular, a very small number of keratohyalin granules, reduced thickness of the epidermis, including a very thin SC, apparent spongiosis, a disturbed corneocyte intracellular matrix, increased outside-in SC permeability, decreased amounts of urocanic and pyrrolidone carboxylic acids, increased UV-B sensitivity, and an altered differentiation program, both at the mRNA and protein levels, were observed. This demonstrates the importance of filaggrin in epidermis homeostasis.

One particularly puzzling modification is the thickness of the RHE. The number of nucleated keratinocyte layers as well as the cellular proliferation rate decreased, but less markedly.

Table 1. Knockdown of filaggrin in reconstructed human epidermis (shFLG RHE) recapitulated some defects observed in the epidermis of *Flg* knockout mice and of IV and AD patients

	shFLG RHE	Flg knockout mice[1]	IV[2]	AD
Hypogranulosis	+	+	+	+
Reduced stratum corneum thickness	+	+/−	−	+/−
Enlargement of extracellular spaces	+	−	−	+
Disturbed corneocyte matrix	+	+	+	+
Increased SC permeability	+	+	+	+
Reduced amounts of urocanic and pyroxylic acids	+	+	+	+
Reduced expression of filaggrin-2 and hornerin	+	Unknown	Unknown	+
Reduced activation of caspase-14	+	Unknown	Unknown	+
Reduced expression of bleomycin hydrolase	+	Unknown	Unknown	+
Reduced expression of loricrin	+	−	−	+
Abnormal expression of tight junction proteins	+	Unknown	+	+
Abnormal corneodesmosome density	+	Unknown	+	Unknown
Increased pH	−	−	+	+

Abbreviations: AD, atopic dermatitis; *Flg*, filaggrin gene; IV, ichthyosis vulgaris; RHE, reconstructed human epidermis; SC, stratum corneum.
[1](Kawasaki *et al.*, 2012).
[2](Gruber *et al.*, 2011).

This difference is therefore probably because of defects in keratinocyte differentiation and proliferation.

Mainly on the basis of *in vitro* or indirect experiments, filaggrin is thought to be essential for the SC, both as a structural protein and as a major source of SC free amino acids, which are highly hygroscopic, absorb part of the UV radiation, and control the SC surface pH (Scott *et al.*, 1982; Rawlings and Harding, 2004; Elias and Steinhoff, 2008; Brown and McLean, 2011). It has been suggested that filaggrin promotes the aggregation of intermediate filaments to form the corneocyte intracellular matrix, and is then degraded within the SC into free amino acids, including large amounts of histidine and glutamine. Histidine and glutamine are further metabolized to urocanic acid and pyrrolidone 5-carboxylic acid, respectively. Urocanic acid was suggested to be involved in skin photoprotection. In support of these possibilities, we have shown that filaggrin knockdown in RHE induces a reduction in pyrrolidone carboxylic and urocanic acids, an increased UV-B-induced apoptosis of keratinocyte, and a disorganized fibrous matrix of corneocytes. The same was observed in recently characterized filaggrin knockout mice (Kawasaki *et al.*, 2012). In addition, filaggrin-deficient epidermis, in both shFLG-RHE and filaggrin knockout mice (Table 1), shows increased penetration of foreign material through the SC—by means of Lucifer yellow in this study and liposome-encapsulated calcein in the mouse study—clearly demonstrating the importance of the protein. However, as observed in the filaggrin-null mice, inhibition of filaggrin expression in RHE does not affect the SC surface pH. This is consistent with a previously published report that filaggrin is not essential for SC acidification (Fluhr *et al.*, 2010). This unexpected result, also observed in filaggrin knockdown three-dimensional skin, has been tentatively explained by compensatory upregulations of the NHE-1 sodium/hydrogen antiporter and sPLA2 secretory phospholipase (Vavrova *et al.*, 2013).

We observed that filaggrin knockdown in RHE significantly influenced keratinocyte differentiation, at both the protein and mRNA levels. Detection of filaggrin-2 and hornerin, two S100-fused type proteins, was decreased. It should be noted that expression of the three proteins appears to be co-regulated *in vivo* and *in vitro* (Pellerin *et al.*, 2013). Caspase-14 and bleomycin hydrolase, two proteases involved in filaggrin degradation, were downregulated, whereas calpain 1 expression was not affected. Two components of cornified cell envelopes were decreased, namely loricrin and the above-mentioned hornerin, suggesting defects in these structures. This is in agreement with the finding that the expression of loricrin is also markedly inhibited in RHE produced with HaCaT cells treated by a small interfering RNA-targeting filaggrin (Yoneda *et al.*, 2012). Finally, in the shFLG RHE, two proteins of cellular junctions, corneodesmosin and claudin 1, are upregulated. These are components of desmosomes/corneodesmosomes and tight junctions, respectively. This suggests the existence of a compensatory mechanism to try to overcome a permeability barrier defect and prevent a more severe phenotype. A similar mechanism has been reported in mice lacking key SC proteins and having a disturbed epidermal barrier (Koch *et al.*, 2000). However, probably because of impaired differentiation, corneodesmosomes were not formed, even though desmosomes appeared normal, and corneodesmosin localization was altered. This may be due to abnormalities in the mechanisms of keratinocyte secretion, lamellar body defects having been described in filaggrin knockdown organotypic skin (Mildner *et al.*, 2010).

In contrast to our observations, Mildner *et al.* (2010) have reported an impairment of the SC diffusion barrier function but normal keratinocyte differentiation and SC morphology when filaggrin is knocked down in human skin equivalents. This difference may be explained by the presence of normal fibroblasts in the collagen matrix they used in Mildner's model. The fibroblasts could partially correct the abnormal keratinocyte phenotype. In models of skin reconstructed *in vitro* and consisting of keratinocytes growing on a scaffold-based dermal equivalent, fibroblasts located in the dermal matrix have already been reported to improve keratinocyte differentiation and sustain epidermal viability (Boehnke *et al.*, 2007). In agreement with our hypothesis, a more recent study using three-dimensional organotypic skin cultures has shown that healthy fibroblasts in the collagen matrix are able to stimulate the expression of filaggrin in atopic keratinocytes (Berroth *et al.*, 2013). This effect could be due to Jun N-terminal kinase-dependent and soluble factors produced by fibroblasts (Schumacher *et al.*, 2014). Several experiments *in vivo* and *in vitro* have also highlighted the leukemia inhibitory factor, a member of the IL-6 family of cytokines whose expression is reduced in atopic skin, as being involved in this process (Berroth *et al.*, 2013).

Many features induced by filaggrin deficiency in RHE have been reported in AD patients (Table 1). These include, in particular, broad defects in epidermal cornification: reduced amount of natural moisturizing factor, altered SC permeability, spongiosis, hypogranulosis, decreased compaction of keratin filaments (Sugiura *et al.*, 2005; Guttman-Yassky *et al.*, 2009; Suarez-Farinas *et al.*, 2011), downregulation of genes encoding loricrin, bleomycin hydrolase, caspase-14, and filaggrin-2 (Sugiura *et al.*, 2005; Guttman-Yassky *et al.*, 2009; Suarez-Farinas *et al.*, 2011), and decreased detection of filaggrin-2, hornerin, caspase-14, bleomycin hydrolase, and loricrin (Broccardo *et al.*, 2011; Kamata *et al.*, 2011; Suarez-Farinas *et al.*, 2011; Pellerin *et al.*, 2013). In addition, in shFLG-RHE we observed a reduction in the conversion rate of procaspase-14 to the active form of the protease. A similar trend has been suggested recently in the epidermis of AD patients, from the study of tape stripping extracts by ELISA (Yamamoto *et al.*, 2011). This prompted us to analyze epidermal extracts of control skin and of both non-lesional and lesional skin of AD patients. Our present data clearly indicate some defect of the caspase-14 activation pathway in AD skin. As caspase-14 deficient mice have shown higher transepidermal water loss, altered filaggrin degradation, and decreased levels of SC free amino acids (Denecker *et al.*, 2008), all characteristics of AD-associated dry skin, it is plausible that reduced amounts of this protease would be involved in the pathogenesis of AD. These data confirm the importance of filaggrin deficiency in AD and suggest that shFLG-RHE is a good *in vitro* model of the epidermal defects caused by the disease.

In conclusion, this study demonstrates that filaggrin deficiency in RHE impairs the epidermal barrier function and reproduces some of the alterations in the epidermal differentiation program observed in AD patients.

MATERIALS AND METHODS

shRNA lentiviral particles

For filaggrin knockdown in keratinocytes, we used MISSION pLKO.1-puro vector–based lentiviral particles containing a puromycin resistance gene and a shRNA insert under the U6 promoter (Sigma-Aldrich, St Louis, MO). Two shRNAs targeting filaggrin exon 3 (shFLG) were tested (shFLGa sequence: (nucleotide position 4934–4954 on the mRNA sequence, NCBI Reference Sequence: NM_002016.1) 5′-CCGGCCAGGTCCCATCAAGAAGATACTCGAGTATCTTCTTGATGGGACCTGGTTTTTG-3′; shFLGb: (nucleotide position 2078–2098) 5′-CCGGGCACTCGTCACACACAGAATTCTCGAGAATTCTGTGTGTGACGAGTGCTTTTTG-3′). A nontarget shRNA that does not target any known human gene (shc) was used as a control (5′-CCGGCAACAAGATGAAGAGCACCAACTC-3′).

Keratinocyte culture and transduction

Primary normal human keratinocytes were obtained from abdominal dermolipectomy of three different healthy subjects who had given their informed consent. They were cultured in Complete DermaLife medium (CellSystems, Troisdorf, Germany) in a humidified atmosphere with 5% CO_2. Keratinocytes were transduced with the lentivirus containing either a shFLG or a nontarget shRNA control at a multiplicity of infection of 10 in the presence of 4 μg ml^{-1} of protamine sulfate. After 24 hours of incubation, the culture medium was replaced with fresh complete medium containing puromycin for selection. When keratinocytes covered 60–70% of the flask area, they were used to produce RHE on polycarbonate filters as described previously (Frankart *et al.*, 2012). More details are available in Supplementary Materials and Methods online.

Immunostaining

On day 10, RHE samples were fixed with 4% formaldehyde-containing buffer and paraffin-embedded. After deparaffinization and hydration, sections were blocked with PBS containing 2% BSA and incubated with primary antibodies (Supplementary Table S1 online). After incubation with the corresponding secondary antibody (Alexa Fluor 555 anti-rabbit IgG, Alexa Fluor 555 or 488 anti-mouse IgG, Alexa Fluor 555 or 488 anti-goat IgG, Invitrogen Life Technologies, Carlsbad, CA), nuclei were stained with 4′,6′-diamidino-2-phenylindole (DAPI; Sigma-Aldrich). The slides were mounted with Mowiol 4–88 (Merck Millipore, Darmstadt, Germany) and observed under a Nikon Eclipse 80i fluorescence microscope equipped with a Nikon DXM 1200C digital camera and NIS image analysis software (Nikon, Tokyo, Japan).

UV radiation

Control and filaggrin knockdown RHE samples were irradiated with 150 mJ cm^{-2} of UV-B (312 nm) using a crosslinker CL-508 (UVItec, Chesterton, UK). Similar RHE samples were treated identically, except for the exposure to UV light. After the treatment, the medium was changed and RHE was further cultivated for 24 hours.

Western blotting

At day 10, RHE was lyzed in 100 μl of Laemmli buffer and boiled twice. Total epidermal proteins were separated on acrylamide gels, and immunodetected with the primary antibodies listed in the Supplementary Table S1 online and with peroxidase-conjugated secondary antibodies (goat anti-rabbit IgG-horseradish peroxidase,

SouthernBiotech, Birmingham, AL; goat anti-mouse IgG-horseradish peroxidase, Bethyl Laboratories, Montgomery, TX). Reaction products were detected by chemiluminescence with the ECL kit (Pierce/Thermo Scientific, Rockford, IL). Quantity One 1-D Analysis Software (Bio-Rad laboratories, Hercules, CA) was used to quantify immunoreactive bands on western blot films after scanning. Signals were normalized to glyceraldehyde 3-phosphate dehydrogenase immunodetection.

Quantitative real-time reverse-transcriptase–PCR

Reverse transcription was performed by using Improm-II Reverse-Transcriptase (Promega, Madison,WI) with a combination of oligo(dT) and random hexamers. Quantitative PCR amplification was performed with the 7300 Real-Time PCR System (Applied Biosystems, Foster City, CA) by using the Sybr quantitative PCR SuperMix W/ROX (Invitrogen Life Technologies). The primers used are listed in the Supplementary Table S2 online. Relative levels of gene expression among samples were determined with the ΔΔ cycle threshold method. TATA box-binding protein gene expression was used for normalization.

Analysis of Lucifer yellow permeability

On day 10, 200 µl of 1 m Lucifer yellow (Sigma-Aldrich) was added onto the SC of the RHE. After incubation at 37 °C for 6 hours, the RHE was fixed in 4% formaldehyde and embedded in paraffin. Sections were inspected under the fluorescence microscope.

Determination of the urocanic acid and pyrrolidone carboxylic acid contents

On day 10, RHE was lyzed in 0.1 M KOH and amino acids were analyzed by HPLC as previously described (Kezic *et al.*, 2009).

Patients and skin samples

Skin biopsies were collected from 15 patients with moderate-to-severe AD (eight female and seven male patients; age 18–45 years; median age 26.5 years) and 20 healthy volunteers (12 female and 8 male controls; age 18–49 years; median age 26.5 years) under institutional review board-approved protocols, and written consent was obtained, as reported previously (Pellerin *et al.*, 2013). Patients and controls were clinically characterized by an experienced dermatologist. All patients underwent punch biopsies on their arms (forearm, antecubital fossa, or wrist), on both lesional and non-lesional skin sites as determined by careful examination of the skin. Biopsies were obtained from controls without any history of atopy at the corresponding skin site. Epidermal proteins were extracted as described (Pellerin *et al.*, 2013) and immunoblotted as described above. *FLG* genotyping was performed in patients and controls for the four *FLG* mutations most prevalent in the European population—R501X, 2282del4, S3247X, and R2447X—using standard and already published methods (Pellerin *et al.*, 2013).

Statistical analysis

Statistical differences were determined with the Student *t*-test (SC properties) and the Mann–Whitney test (caspase-14 activation and amounts). A value of $P<0.05$ was considered statistically significant.

CONFLICT OF INTEREST

The authors state no conflict of interest.

ACKNOWLEDGMENTS

We are indebted to Jean-Pierre Chavoin (Department of Plastic Surgery, Hospital of Toulouse, France) for the human skin samples and to Jens-Michael Schröder (University-Hospital Schleswig-Holstein, Kiel, Germany) for his kind gift of anti-filaggrin-2 antibodies. We thank Renan Destrade and Carole Pons for their excellent technical assistance, Sophie Allart and Astrid Canivet from the cellular imaging facility (INSERM UMR 1043, Toulouse Rio Imagerie, Toulouse), and Bruno Payré from the Electron Microscopy facility (the University of Toulouse, Toulouse Rio Imagerie). We thank Daniel Redoules (Pierre Favre Dermo-Cosmétique, Toulouse, France) for the loan of the pH meter used to evaluate the RHE surface pH. This work was supported by the French National Center for Scientific Research (CNRS), Toulouse University, the French National Institute of Health and Medical Research (INSERM), the European COST program ''SKINBAD'' (action BM0903) and the French Society for Dermatology (Société Française de Dermatologie). L Pellerin was supported by the ''Fondation pour la Dermatite Atopique''.

SUPPLEMENTARY MATERIAL

Supplementary material is linked to the online version of the paper at http://www.nature.com/jid

REFERENCES

Aho S, Harding CR, Lee JM *et al.* (2012) Regulatory role for the profilaggrin N-terminal domain in epidermal homeostasis. *J Investig Dermatol Symp Proc* 132:2376–85

Barresi C, Stremnitzer C, Mlitz V *et al.* (2011) Increased sensitivity of histidinemic mice to UVB radiation suggests a crucial role of endogenous urocanic acid in photoprotection. *J Investig Dermatol Symp Proc* 131:188–94

Baurecht H, Irvine AD, Novak N *et al.* (2007) Toward a major risk factor for atopic eczema: meta-analysis of filaggrin polymorphism data. *J Allergy Clin Immunol* 120:1406–2

Berroth A, Kuhnl J, Kurschat N *et al.* (2013) Role of fibroblasts in the pathogenesis of atopic dermatitis. *J Allergy Clin Immunol* 131:1547–54. e6

Bieber T (2012) Atopic dermatitis 2.0: from the clinical phenotype to the molecular taxonomy and stratified medicine. *Allergy* 67:1475–82

Boehnke K, Mirancea N, Pavesio A *et al.* (2007) Effects of fibroblasts and microenvironment on epidermal regeneration and tissue function in long-term skin equivalents. *Eur J Cell Biol* 86:731–46

Boguniewicz M, Leung DY (2011) Atopic dermatitis: a disease of altered skin barrier and immune dysregulation. *Immunol Rev* 242:233–46

Broccardo CJ, Mahaffey S, Schwarz J *et al.* (2011) Comparative proteomic profiling of patients with atopic dermatitis based on history of eczema herpeticum infection and Staphylococcus aureus colonization. *J Allergy Clin Immunol* 127:186–93. 93 e1-11

Brown SJ, McLean WH (2011) One remarkable molecule: filaggrin. *J Investig Dermatol Symp Proc* 132:751–62

Chavanas S, Mechin MC, Nachat R *et al.* (2006) Peptidylarginine deiminases and deimination in biology and pathology: relevance to skin homeostasis. *J Dermatol Sci* 44:63–72

Cork MJ, Robinson DA, Vasilopoulos Y *et al.* (2006) New perspectives on epidermal barrier dysfunction in atopic dermatitis: gene-environment interactions. *J Allergy Clin Immunol* 118:3–21

Dale BA, Resing KA, Lonsdale-Eccles JD (1985) Filaggrin: a keratin filament associated protein. *Ann N Y Acad Sci* 455:330–42

Dapic I, Jakasa I, Nico LHY *et al.* (2013) Evaluation of an HPLC method for the determination of natural moisturizing factors in the human stratum corneum. *Anal Lett* 46:2133–44

Denecker G, Ovaere P, Vandenabeele P *et al.* (2008) Caspase-14 reveals its secrets. *J Cell Biol* 180:451–8

Elias PM, Steinhoff M (2008) "Outside-to-inside" (and now back to "outside") pathogenic mechanisms in atopic dermatitis. *J Investig Dermatol Symp Proc* 128:1067–70

Fluhr JW, Elias PM, Man MQ *et al.* (2010) Is the filaggrin-histidine-urocanic acid pathway essential for stratum corneum acidification? *J Investig Dermatol Symp Proc* 130:2141–4

Frankart A, Malaisse J, De Vuyst E *et al.* (2012) Epidermal morphogenesis during progressive in vitro 3D reconstruction at the air-liquid interface. *Exp Dermatol* 21:871–5

Gruber R, Elias PM, Crumrine D *et al.* (2011) Filaggrin genotype in ichthyosis vulgaris predicts abnormalities in epidermal structure and function. *Am J Pathol* 178:2252–63

Guttman-Yassky E, Suarez-Farinas M, Chiricozzi A *et al.* (2009) Broad defects in epidermal cornification in atopic dermatitis identified through genomic analysis. *J Allergy Clin Immunol* 124:1235–44. e58

Ishida-Yamamoto A, Takahashi H, Presland RB *et al.* (1998) Translocation of profilaggrin N-terminal domain into keratinocyte nuclei with fragmented DNA in normal human skin and loricrin keratoderma. *Lab Invest* 78:1245–53

Jungersted JM, Scheer H, Mempel M *et al.* (2010) Stratum corneum lipids, skin barrier function and filaggrin mutations in patients with atopic eczema. *Allergy* 65:911–8

Kamata Y, Yamamoto M, Kawakami F *et al.* (2011) Bleomycin hydrolase is regulated biphasically in a differentiation- and cytokine-dependent manner: relevance to atopic dermatitis. *J Biol Chem* 286:8204–12

Kawasaki H, Nagao K, Kubo A *et al.* (2012) Altered stratum corneum barrier and enhanced percutaneous immune responses in filaggrin-null mice. *J Allergy Clin Immunol* 129:1538–46. e6

Kezic S, Kammeyer A, Calkoen F *et al.* (2009) Natural moisturizing factor components in the stratum corneum as biomarkers of filaggrin genotype: evaluation of minimally invasive methods. *Br J Dermatol* 161: 1098–104

Kezic S, Kemperman PM, Koster ES *et al.* (2008) Loss-of-function mutations in the filaggrin gene lead to reduced level of natural moisturizing factor in the stratum corneum. *J Investig Dermatol Symp Proc* 128:2117–9

Kezic S, Novak N, Jasaka I *et al.* (2014) Skin barrier in atopic dermatitis. *Front Biosci* 19:542–6

Koch PJ, de Viragh PA, Scharer E *et al.* (2000) Lessons from loricrin-deficient mice: compensatory mechanisms maintaining skin barrier function in the absence of a major cornified envelope protein. *J Cell Biol* 151:389–400

Mildner M, Jin J, Eckhart L *et al.* (2010) Knockdown of filaggrin impairs diffusion barrier function and increases UV sensitivity in a human skin model. *J Investig Dermatol Symp Proc* 130:2286–94

Novak N, Simon D (2011) Atopic dermatitis—from new pathophysiologic insights to individualized therapy. *Allergy* 66:830–9

Odhiambo JA, Williams HC, Clayton TO *et al.* (2009) Global variations in prevalence of eczema symptoms in children from ISAAC Phase Three. *J Allergy Clin Immunol* 124:1251–8. e23

Oyoshi MK, He R, Kumar L *et al.* (2009) Cellular and molecular mechanisms in atopic dermatitis. *Adv Immunol* 102:135–226

Pearton DJ, Dale BA, Presland RB (2002) Functional analysis of the profilaggrin N-terminal peptide: identification of domains that regulate nuclear and cytoplasmic distribution. *J Investig Dermatol Symp Proc* 119:661–9

Pellerin L, Henry J, Hsu CY *et al.* (2013) Defects of filaggrin-like proteins in both lesional and nonlesional atopic skin. *J Allergy Clin Immunol* 131:1094–2

Rawlings AV, Harding CR (2004) Moisturization and skin barrier function. *Dermatol Ther* 17(Suppl 1):43–8

Rodriguez E, Baurecht H, Herberich E *et al.* (2009) Meta-analysis of filaggrin polymorphisms in eczema and asthma: robust risk factors in atopic disease. *J Allergy Clin Immunol* 123:1361–70. e7

Schumacher M, Schuster C, Rogon ZM *et al.* (2014) Efficient keratinocyte differentiation strictly depends on JNK-induced soluble factors in fibroblasts. *J Investig Dermatol Symp Proc* 134:1332–41

Scott IR, Harding CR, Barrett JG (1982) Histidine-rich protein of the keratohyalin granules. Source of the free amino acids, urocanic acid and pyrrolidone carboxylic acid in the stratum corneum. *Biochim Biophys Acta* 719:110–7

Steinert PM, Cantieri JS, Teller DC *et al.* (1981) Characterization of a class of cationic proteins that specifically interact with intermediate filaments. *Proc Natl Acad Sci USA* 78:4097–101

Suarez-Farinas M, Tintle SJ, Shemer A *et al.* (2011) Nonlesional atopic dermatitis skin is characterized by broad terminal differentiation defects and variable immune abnormalities. *J Allergy Clin Immunol* 127:954–64. e1-4

Sugiura H, Ebise H, Tazawa T *et al.* (2005) Large-scale DNA microarray analysis of atopic skin lesions shows overexpression of an epidermal differentiation gene cluster in the alternative pathway and lack of protective gene expression in the cornified envelope. *Br J Dermatol* 152:146–9

Vavrova K, Henkes D, Struver K *et al.* (2013) Filaggrin deficiency leads to impaired lipid profile and altered acidification pathways in a 3D skin construct. *J Investig Dermatol Symp Proc* 134:746–53

Winge MC, Hoppe T, Berne B *et al.* (2011) Filaggrin genotype determines functional and molecular alterations in skin of patients with atopic dermatitis and ichthyosis vulgaris. *PLoS One* 6:e28254

Yamamoto M, Kamata Y, Iida T *et al.* (2011) Quantification of activated and total caspase-14 with newly developed ELISA systems in normal and atopic skin. *J Dermatol Sci* 61:110–7

Yoneda K, Nakagawa T, Lawrence OT *et al.* (2012) Interaction of the profilaggrin N-terminal domain with loricrin in human cultured keratinocytes and epidermis. *J Investig Dermatol Symp Proc* 132:1206–4

SUPPLEMENTARY MATERIALS AND METHODS

Keratinocyte culture and transduction

Primary normal human keratinocytes were obtained from abdominal dermolipectomy of 3 different healthy subjects who had given their informed consent. They were cultured in Complete DermaLife medium (CellSystems, Troisdorf, Germany), supplemented as recommended by the manufacturer and containing 50 IU/ml penicillin and 50 mg/ml streptomycin (Invitrogen Life Technologies, Carlsbad, CA). Keratinocytes were transduced with the lentivirus containing either a shFLG or the non-target shRNA control at a multiplicity of infection of 10 in the presence of 4 µg/ml of protamine sulfate. After 24 hours of incubation, the culture medium was replaced with fresh complete medium containing puromycin for selection. When keratinocytes covered 60-70% of the flask area, they were used to produce RHE on polycarbonate filters as described previously (Frankart *et al.*, 2012). Briefly, cells were harvested by trypsinization, pelleted for 5 min at 1200 rpm at 4°C, and resuspended at a density of 700 000 cells/ml in ice-cold EpiLife medium (Invitrogen Life Technologies) containing 1.5 mM calcium. Polycarbonate culture inserts (area of 0.63 cm^2 with pores 0.4 µm in diameter; Merck Millipore, Billerica, MA) were placed in six-well plates containing 2.5 ml of cold medium. Each insert received 500 µl of keratinocyte suspension corresponding to 500 000 cells/cm^2. After 24 h of incubation at 37°C in a humidified atmosphere containing 5% CO2, cells were exposed to the air–liquid interface by removing the medium in the upper compartment. The 2.5 ml of medium under the filter were replaced by 1.5 ml of complete EpiLife medium, supplemented with 1.5 mM calcium, 50 µg/ml of vitamin C (Sigma-Aldrich) and 10 ng/ml of keratinocyte growth factor (Sigma-Aldrich). The medium was renewed every 2 days during the 10 days of air–liquid interface culture.

Transmission electron microscopy

Samples were fixed with 2.5% glutaraldehyde-formaldehyde buffer (sodium cacodylate 0.1M, pH 7.4) for 6 hours, washed with Sorensen phosphate buffer (0.2 M) for 12 hours. Then they were post-fixed with 1% OsO_4 in Sorensen buffer (phosphate 0.05 M, glucose 0.25 M) for 1 hour. Samples were dehydrated in an ascending ethanol series up to ethanol 100% and then with propylene oxide. They were embedded in epoxy resin (Epon 812). After 24 hours of polymerization at 60°C, ultrathin

sections (70 nm thick) were mounted on 100-mesh collodion-coated copper grids and post-stained with 3% uranyl acetate in 50% ethanol and with 8.5% lead citrate before being examined on an HT7700 Hitachi electron microscope at an accelerating voltage of 80 kV.

Morphological analysis

Epidermal thickness, number of keratinocyte layers and number of cells per 100 µm of tissue length were assessed using images of hematoxylin-eosin stained sections of paraffin embedded reconstructed human epidermis (RHE), counting three fields per slide. Experiments were performed with keratinocytes from three individuals. Keratohyalin granules were counted on electron microscopy images of reconstructed human epidermis produced with keratinocytes from one individual. Statistical significance was tested using the Student's *t*-test.

Cell Viability assay

Cell viability was determined by using a MTT (3-(4,5-dimethylthiazol-2-yl)-2,5-diphenyltetrazolium bromide; Sigma-Aldrich) reduction assay. Each RHE was incubated for 1 h at 37°C in 500 µl of MTT (0.5 mg/ml). Formazan crystals were extracted in 0.5 ml of isopropanol, and the absorbance at 550 nm was recorded using a microplate reader. Topical application of a 3% solution of SDS on the surface of the RHE was used as a positive control.

Table S1: primary antibodies.

Antigen	Clone n° / name	Company	Dilution
Filaggrin	AHF3	Home made[1]	1:25000
Filaggrin 2	Polyclonal αhIFPS2	J-M Schroeder[2]	1:1000
Hornerin	Polyclonal HPA031469	Sigma-Aldrich	1:500
GAPDH	6C5	Santa Cruz Biotechnology	1:500
Involucrin	SY5	Sigma-Aldrich	1:1000
Loricrin	AF62	Covance	1:10000
Desmocollin 1	Dsc1-U100	Research Diagnostic Inc.	1:50
Desmoglein 1/2	DG 3.10	Progen	1:500
Claudin 1	1C5-D9	Sigma-Aldrich	1:500
Keratin 10	LH2	Santa Cruz Biotechnology	1:32000
Keratin 14	C8791	Sigma-Aldrich	1:500
Bleomycin hydrolase	Polyclonal HPA039548	Sigma-Aldrich	1:1000
Caspase 14	D-10	Santa Cruz Biotechnology	1:100
Calpain 1	Polyclonal HPA005992	Sigma-Aldrich	1:250
Corneodesmosin	F28-27	Home made[3]	1:1000
E-cadherin	Clone 36	BD Transduction laboratories	1:2500
Ki67	Ab16667	Abcam	1:100
Active caspase-3	AF835	R&D systems	1:500

[1]Simon M, Sebbag M, Haftek M, Vincent C, Girbal-Neuhauser E, Rakotoarivony J, et al. Monoclonal antibodies to human epidermal filaggrin, some not recognizing profilaggrin. J Invest Dermatol 1995; 105:432-7. [2]Wu Z, Hansmann B, Meyer-Hoffert U, Glaser R, Schroder J- M. Molecular identification and expression analysis of filaggrin-2, a member of the S100 fused-type protein family. PLoS One 2009; 4:e5227. [3]Guerrin M, Simon M, Montézin M, Haftek M, Vincent C, Serre G. Expression cloning of human corneodesmosin proves its identity with the product of the S gene and allows improved characterization of its processing during keratinocyte differentiation. J Biol Chem 1998; 273:22640-7.

Table S2: Sequences of qPCR primers

Gene	Forward	Reverse
FLG	5'-GCAAGGTCAAGTCCAGGAGAA-3'	5'-CCCTCGGTTTCCACTGTCTC-3'
FLG2	5'-TCTGAAGAACCCAGATGATCCA-3'	5'-CATCAAAAGAAACTCAGTAAAGTCCAA-3'
HRNR	5'-AGGACAGGGCTATAGTCAGCA-3'	5'-CCGAAGCGTGATGGGAGG-3'
IVL	5'-GGGTGGTTATTTATGTTTGGGTGG-3'	5'-GCCAGGTCCAAGACATTCAAC-3'
LOR	5'-CGAAGGAGTTGGAGGTGTTT-3'	5'-ACTGGGGTTGGGAGGTAGTT-3'
DSC1	5'-CATGGGTGGTCAGCCTTTCGGT-3'	5'-TCCTGATCCTGTACCTTCATTGGCA-3'
DSG1	5'-GAAGGCAGAAACGTGAATGGA-3'	5'-TTTTGGCGATTGGGTTCCT-3'
CLDN1	5'-TGGCATGAAGTGTATGAAGTGCTT-3'	5'-CCCCAATGACAGCCATCCT-3'
K10	5'-TGATGTGAATGTGGAAATGAATGC-3'	5'-GTAGTCAGTTCCTTGCTCTTTTCA-3'
K14	5'-CTCATCCTCCCGCTTCTCCT-3'	5'-AAAGCCACTACCAAAGCTGCT-3'
BLMH	5'-GTGGTGGACAGGAAGCATGT-3'	5'-TCCTTTGCAGCTACGTCAGG-3'
CASP14	5'-TGCACGTTTATTCCACGGTA-3'	5'-TGCTTTGGATTTCAGGGTTC-3'
CAPN1	5'-CAAACACCCCTCCCCCAGGATGT-3'	5'-CGCACCCGCAGCTGCTCATA-3'
CDSN	5'-ACTGCTGCTGGCTGGTCT-3'	5'-AGAGCTTCTGGCACTGGAAA-3'
CDH1	5'-CTGCTGCTCTTGCTGTTTCTTC-3'	5'-CTCCGCCTCCTTCTTCATCATA-3'
TBP	5'-TCAAACCCAGAATTGTTCTCCTTAT-3'	5'-CCTGAATCCCTTTAGAATAGGGTAGA-3'

SUPPLEMENTARY FIGURES

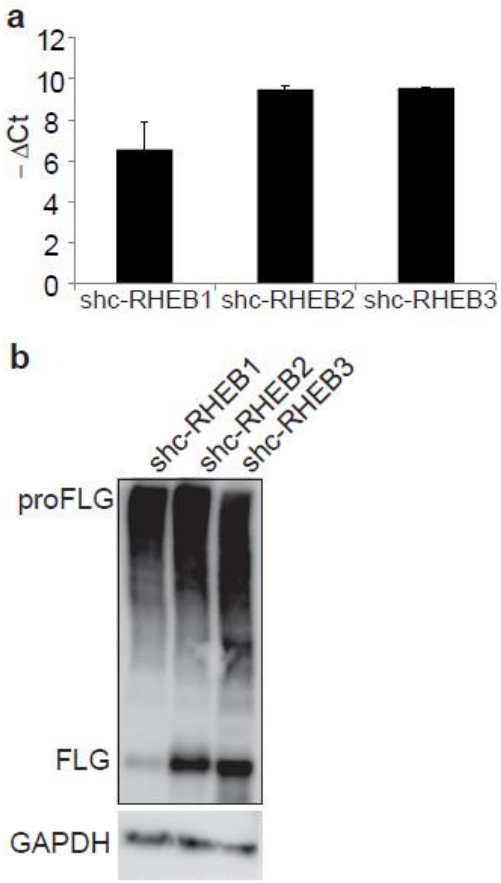

Figure S1. Expression of filaggrin in RHE produced with keratinocytes from three individuals. Fully differentiated shc-RHE were analyzed by qRT-PCR (**a**), and Western blotting performed with anti-filaggrin AHF3 antibody (**b**).

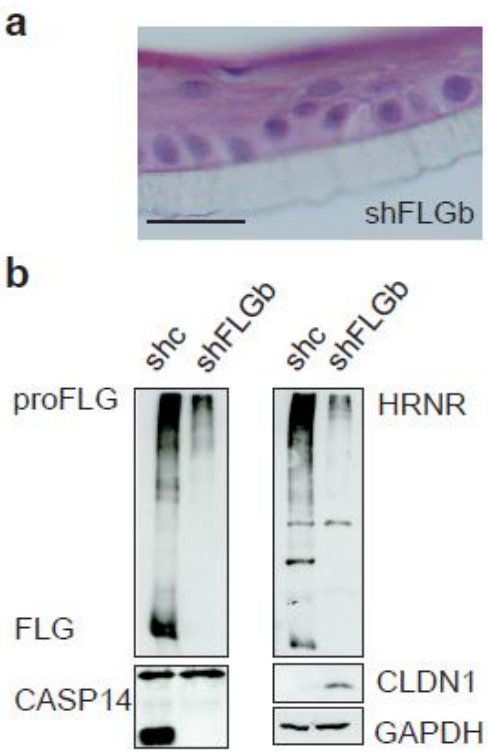

Figure S2. In RHE produced with shFLGb-treated keratinocytes, expression of filaggrin was highly reduced, epidermal morphology was altered, and keratinocyte differentiation was impaired. (a) Sections of paraffin-embedded shFLGb-RHE were stained with hematoxylin and eosin. Bar = 20 µm. **(b)** Fully differentiated shc- and shFLGb-RHE were analyzed by Western blotting performed with anti-filaggrin (FLG), -hornerin (HRNR), -GAPDH, claudin-1 (CLDN1) and caspase-14 (CASP14) antibodies.

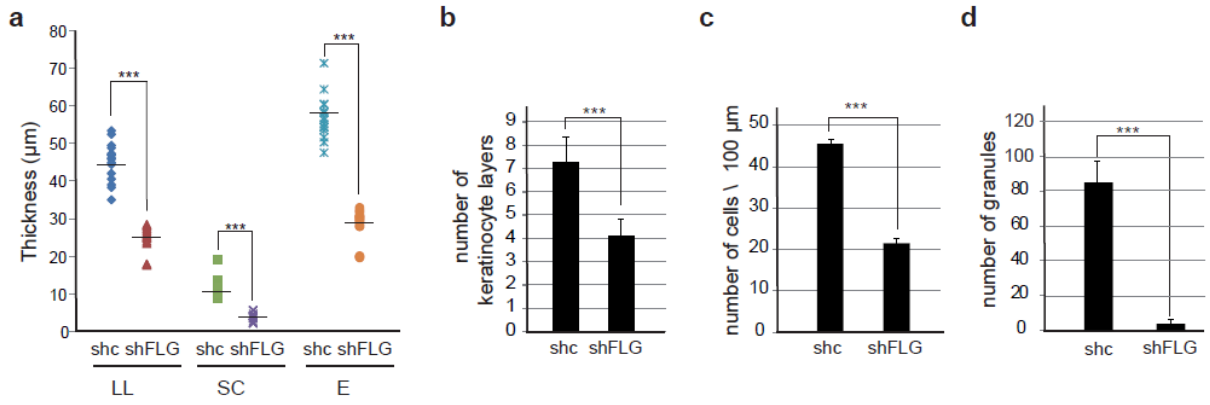

Figure S3. Quantification of morphological changes in filaggrin knockdown RHE. (**a-c**) Sections of paraffin-embedded shc- and shFLG-RHE were stained with hematoxylin and eosin. Thickness of the living keratinocyte layers (from stratum basale to stratum granulosum; LL) and of the *stratum corneum* (SC) and total epidermal thickness (E) were measured (**a**). Number of keratinocyte layers (**b**) and number of nucleated keratinocytes per 100 µm length of tissue (**c**) were counted. (**d**) Identical RHE were analyzed by electron microscopy, and keratohyalin granules were counted and are indicated as number per surface unit. ***P < 0.001.

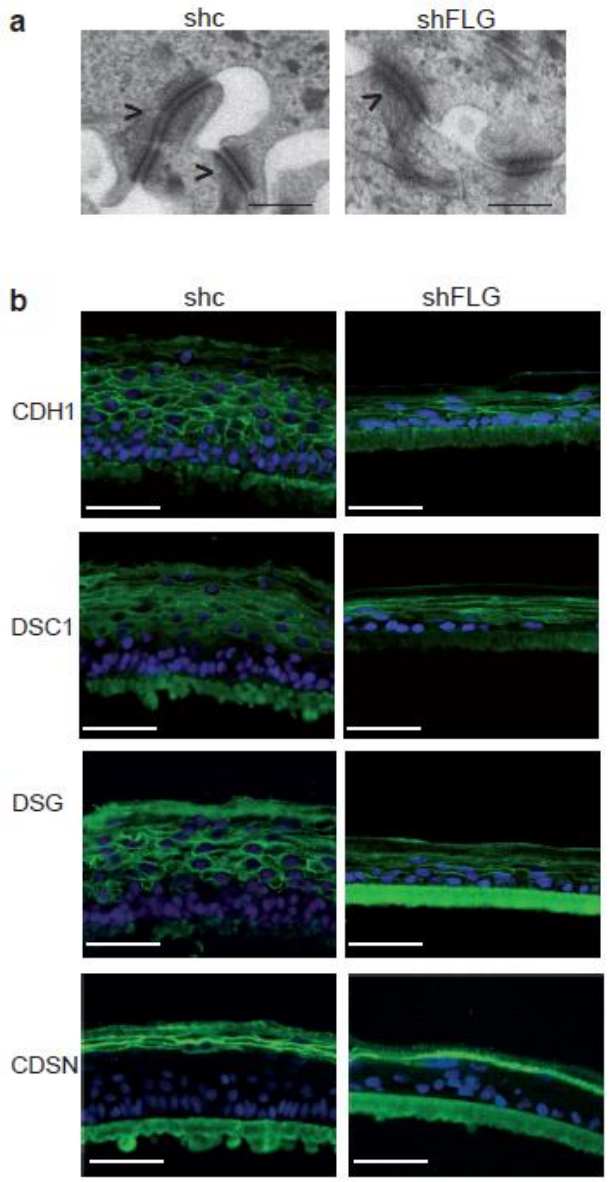

Figure S4. In filaggrin knockdown RHE desmosomes and the distribution of junction proteins, except corneodesmosin, appeared normal. Shc- and shFLG-RHE were analyzed by electron microscopy (**a**) and indirect immunofluorescence with antibodies specific for E-cadherin (CDH1), desmocollin 1 (DSC1), desmoglein 1/2 (DSG) and corneodesmosin (CDSN) (**b**). Desmosomes of upper keratinocytes (arrowheads) are indicated. Bars = 250 nm (a) and 50 µm (b).

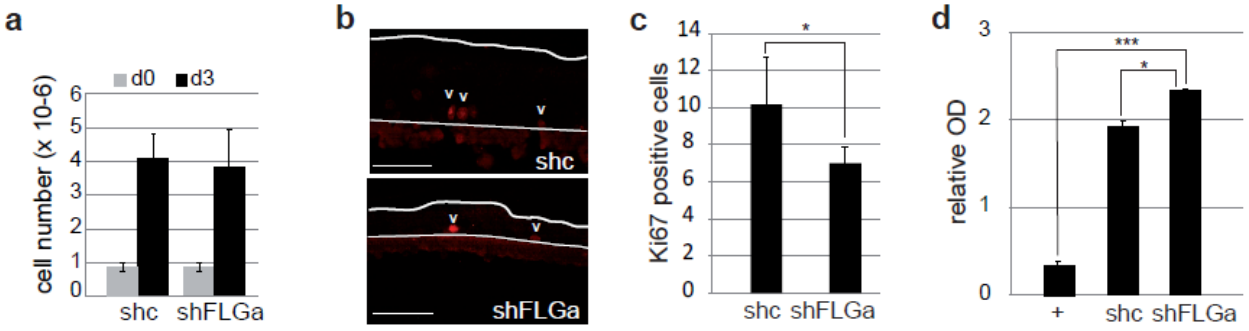

Figure S5. Filaggrin knockdown modified the keratinocyte proliferation rate but did not induce cellular death. (**a**) Equal number of shc- and shFLGa-treated keratinocytes ($1x10^6$ cells) were seeded in 150 cm² flasks at day 0 (d0) and cultured in Complete DermaLife medium for three days. At day 3 (d3) cells were counted. (**b**) Staining of Ki67 in keratinocytes (arrowheads) of the basal and immediate suprabasal layers of shc- and shFLGa-RHE at day 10. The thick and thin lines indicate the stratum corneum surface and the epidermis/polycarbonate membrane junction, respectively. Bars = 50 µm. (**c**) The number of Ki67 positive cells was quantified and is indicated per RHE length unit. (**d**) Cell viability of Shc- and shFLGa-RHE at day 10 was measured by MTT assay. The toxic effect of a 3% SDS solution on the shc-RHE was used as a control (+). Results are expressed as mean ± S.D. of at least three independent determinations. *, $p < 0.05$; ***, $p < 0.001$.

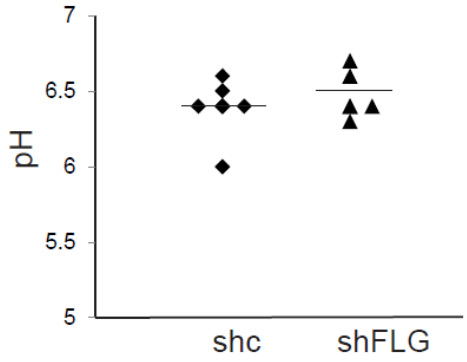

Figure S6. In filaggrin knockdown RHE the superficial stratum corneum pH was not modified.

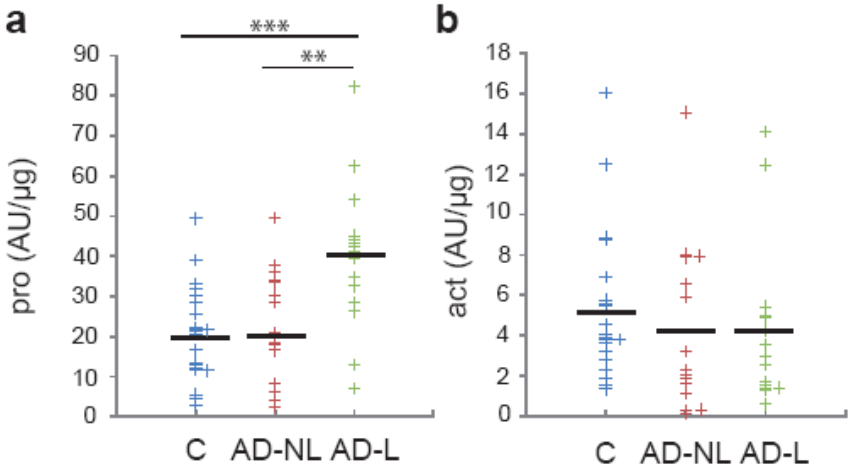

Figure S7. Detection of procaspase-14 and of the activated form of caspase-14 in normal and atopic skin. Equal volumes of epidermal extracts of 20 control healthy subjects (C) and 15 patients with atopic dermatitis (AD) were analyzed by Western blotting with an antibody recognizing both the proform and the large subunit of caspase-14. Both the non-lesional (NL) and lesional (L) skin were analyzed. The immunodetected procaspase-14 (pro) and large subunit of active caspase-14 (act) were quantified, normalized to the total amounts of proteins in the samples and plotted as arbitrary units (AU) per µg of proteins for each of the extracts. Bars represent the mean values; **, $p < 0.01$; ***, $p < 0.001$.

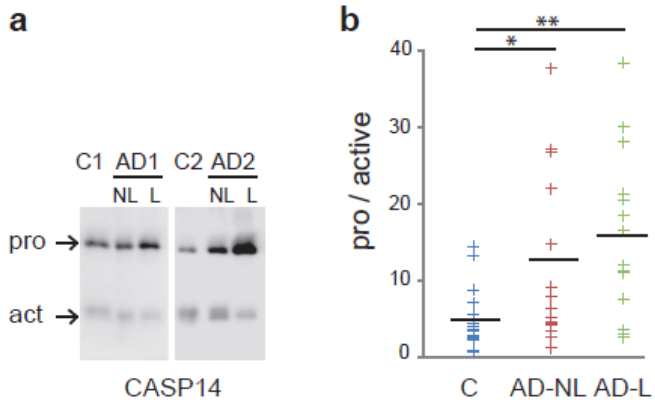

Figure S8. Procaspase-14 activation was reduced in atopic skin.

Equal volumes of epidermal extracts of 20 control healthy subjects (C) and 15 patients with atopic dermatitis (AD) were analyzed by Western blotting with an antibody recognizing both the proform and the large subunit of caspase-14. (**a**) Representative results corresponding to the extracts of two controls (C1 and C2), and of two patients (AD1 and AD2). Both the non-lesional (NL) and lesional (L) skin were analyzed. The detected procaspase-14 (pro) and large subunit of active caspase-14 (act) are indicated. (**b**) The immunodetected bands were quantified, and the ratio procaspase-14/active caspase-14 plotted for each of the extracts. Bars represent the mean values; *, $p = 0.0437$; **, $p = 0.00163$.